

## Phytoplanktonic biomass synthesis: application to deviations from Redfield stoichiometry\*

FERNANDO FRAGA

Instituto de Investigaciones Marinas, Consejo Superior de Investigaciones Científicas, Eduardo Cabello 6, 36208 Vigo, Spain.

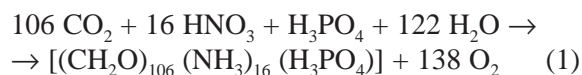
**SUMMARY:** During biomass formation as a result of phytoplankton photosynthesis, CO<sub>2</sub> and the nutrients NO<sub>3</sub> and PO<sub>4</sub> are consumed and O<sub>2</sub> produced in fixed proportions known as the Redfield ratio. Broecker's tracers, i.e., "NO" = O<sub>2</sub>+R<sub>N</sub>·NO<sub>3</sub>, "PO" = O<sub>2</sub>+R<sub>P</sub>·PO<sub>4</sub>, and "CO" = O<sub>2</sub>+R<sub>C</sub>·CO<sub>2</sub>, remain constant during photosynthesis, because nutrients consumed are offset by O<sub>2</sub> formation. When one or several nutrients become depleted, the Redfield ratio no longer holds, and the tracers cease to remain constant. The main causes are formation of excess carbohydrates or lipids, N<sub>2</sub> fixation, or production of CaCO<sub>3</sub> plates by phytoplanktonic populations that have developed different strategies for obtaining the nutrients they need. This paper presents new tracers that remain constant, irrespective of whether or not Redfield stoichiometry is satisfied. Differences between the values of the new tracers and the values of the conventional tracers reveal the presence of anomalies in biomass production. They also allow quantification of any such anomalies, both globally and by depth stratum, and assessment of each individual anomaly separately, even when more than one anomaly occur simultaneously.

*Key words:* Redfield deviations, phytoplankton stoichiometry, dinoflagellates, coccolithophores, cyanobacteria.

### INTRODUCTION

Organic matter making up the marine phytoplankton is composed primarily of proteins, carbohydrates, lipids, nucleic acids, and photosynthesizing pigments. All these constituents consist of carbon, oxygen, and hydrogen atoms, and additionally the proteins and photosynthesizing pigments contain nitrogen and the nucleic acids contain nitrogen and phosphorus. The phytoplankton takes all these elements from the sea water, where they are present in mineral form. Using their own data on the proximal composition of the plankton together with data published by Fleming (1940), Redfield *et al.* (1963)

established the -O<sub>2</sub>:C:N:P ratio of 138:106:16:1 based on the finding that the phytoplankton reduced CO<sub>2</sub> to carbohydrates and nitrate to ammonia according to the following stoichiometric equation:



This equation holds true for carbohydrate synthesis and provides a good approximation for protein synthesis, but it should be kept in mind that a large proportion, between 12 and 22%, is in the form of lipids, in which the carbon is in a less highly oxidized state than it is in the carbohydrates, and hence the amount of O<sub>2</sub> produced is actually higher than the quantity estimated by Equation 1. Thus, ratios of

\*Received February 25, 2001. Accepted June 27, 2001.

O<sub>2</sub> to C, N, and P must be higher. Despite this limitation, Equation 1 has been used quite successfully and is still employed by many researchers today.

The elemental composition of the phytoplankton is relatively uniform as long as the sea water contains sufficient amounts of the nutrient salts NO<sub>3</sub><sup>-</sup>, HPO<sub>4</sub><sup>2-</sup>, and H<sub>4</sub>SiO<sub>4</sub>. However, when one or more nutrients are depleted, the phytoplankton may exhibit abnormal behaviour in respect of nutrient usage, and indeed the species ordinarily present may even be replaced by other species that are better able to obtain the nutrients needed for growth (Margalef, 1978), and the conditions for the Redfield ratio are no longer fulfilled, with the resulting impact on the stoichiometry of nutrients and oxygen. These anomalies not only allow us to determine what has taken place but also make it possible to quantify all the deviations.

The anomalies most commonly encountered in the photic layer include excess carbohydrate synthesis, a generalized phenomenon among populations that have been aged by nutrient deficiency (Williams, 1995), sometimes giving rise to quite striking situations of gelatinous polysaccharide formation (Vollenweider *et al.*, 1995). On other occasions the anomalies lead to blooms of dinoflagellates or organisms like the photosynthetic ciliate *Mesodinium*, able to carry out vertical migrations into the photic zone, where they synthesize carbohydrates, and then down to the subphotic zone at dusk, where they take in nutrients and synthesize proteins and nucleic acids from the carbohydrates before returning back to the photic zone (Cullen, 1985; Cullen *et al.*, 1985; Fraga *et al.*, 1992, 1999). Certain large diatoms employ a similar strategy to obtain NO<sub>3</sub><sup>-</sup>, employing a pattern of passive vertical migration as a result of density variations caused by accumulation of carbohydrates (Moore and Villareal, 1996; Richardson *et al.*, 1996; Villareal *et al.*, 1996; Richardson *et al.*, 1998; Villareal *et al.*, 1999).

Silicate impoverishment also produces anomalies. While variations in Si(OH)<sub>4</sub> do not in themselves affect the -ΔO<sub>2</sub>:ΔC ratio, diatoms accumulate lipids as a result of silicate depletion (Taguchi *et al.*, 1987), thus altering the stoichiometry of photosynthesis.

When it is nitrogen, not phosphorus, in the nutrient supply that is depleted, cyanobacteria that are able to use dissolved N<sub>2</sub> gas in the sea water as a nitrogen source enjoy an advantage. Since they are using an unoxidized form of nitrogen, oxygen production is lower.

Coccolithophores are another group of organisms that can grow in nutrient-poor environments and can cause profound alterations in the stoichiometry of carbon through coccolith, or calcite plate, formation (Paasche, 1998). Other CaCO<sub>3</sub>-fixing organisms have a similar effect.

## AVERAGE PHYTOPLANKTON COMPOSITION

The composition of the plankton can be extremely variable, depending on the species present locally and on prevailing environmental conditions. These differences are the result of variable proportions among proteins, nucleic acids, carbohydrates, and lipids. Still, each of these groups has a quite constant elemental composition, i.e., a sample may contain a high or a low amount of protein, but the elemental composition of that protein will remain practically invariable.

Table 2, taken from Fraga and Pérez (1990), gives the composition of each of these groups. This Table shows that the largest difference in the ratio of oxygen to carbon is between the carbohydrates and the lipids, and hence the relative proportions of these two groups of biomolecules are of most importance in calculating the oxygen content in the elemental composition of the phytoplankton.

The initial atomic C:N:P ratio and the carbohydrate:lipid ratio, Q<sub>CL</sub>, expressed as number of carbon atoms, can be used as a basis for a system of relations for calculating the average phytoplankton composition, based on chemical formulas 2, 3, 4 and 7 in Table 2.

TABLE 1. – List of commonly used abbreviations

A <sub>p</sub>	= Potential alkalinity (see Eq. 10)
A <sub>T</sub>	= Total alkalinity
C-Cbh	= Carbohydrates, expressed as moles of carbon
C-Red	= Organic carbon produced according to Redfield stoichiometry (Eq. 2)
CO <sub>2</sub> <sup>o</sup>	= Total preformed inorganic carbon
C <sub>T</sub>	= Total dissolved inorganic carbon (DIC)
NO <sub>3</sub> <sup>o</sup>	= Preformed nitrate (see Eq. 5)
Q <sub>CL</sub>	= Carbohydrate:lipid ratio, expressed as atoms of carbon
R <sub>C</sub>	= -ΔO <sub>2</sub> :ΔC, in moles
R <sub>CS</sub>	= R <sub>C</sub> for reserves: Carbohydrates, R <sub>CS</sub> = 1; lipids, R <sub>CS</sub> = 1.36
R <sub>N</sub>	= -ΔO <sub>2</sub> :ΔN, in moles
R <sub>N</sub> /R <sub>C</sub>	= C:N, in moles
R <sub>P</sub>	= -ΔO <sub>2</sub> :ΔP, in moles
Z <sub>C</sub>	= Compensation depth at which carbohydrate synthesis is equal to carbohydrate usage
Z <sub>D</sub>	= Depth at which biological activity no longer results in perturbation of Redfield stoichiometry
"XO"	= Any tracer from Table 4
"XO" <sub>D</sub>	= Value of "XO" at Z <sub>D</sub>
Δ"XO" <sub>D</sub>	= "XO" - "XO" <sub>D</sub>

TABLE 2. – Mean proximate composition for each group of biomolecules making up the marine phytoplankton and the respective  $R_C$ ,  $R_N$ , and  $R_P$  values, expressing moles of  $O_2$  consumed for complete oxidation of the C, N, or P atoms respectively.

	Mean atomic formula <sup>1</sup>	$R_C$	$R_N$	$R_P$
Carbohydrates <sup>2</sup>	$C_{17}H_{28}O_{14}$	1.00		
Lipids <sup>3</sup>	$C_{53}H_{89}O_6$	1.36		
Phosphorus compounds <sup>4</sup>	$C_{45}H_{76}O_{31}N_{12}P_5$	1.55	5.81	13.95
Proteins <sup>5</sup>	$C_{138}H_{217}O_{45}N_{39}S$	1.59	5.64	
Chlorophylls <sup>6</sup>	$C_{46}H_{52}O_5N_4Mg$	1.35	15.50	
Proteins + Chlorophylls <sup>7</sup>	$C_{147}H_{227}O_{46}N_{40}S Mg_{0.16}$	1.58	5.80	
Proteins + Chlorophylls + Phosphorus compounds <sup>8</sup>	$C_{177}H_{277}O_{66}N_{48}P_3 S Mg_{0.16}$	1.57	5.80	92.86

(1) The atomic formulas shown do not correspond to any chemical molecule but are instead the mean ratio of atoms for all compounds in each group of biomolecules

(2) Comprising 83% hexoses, 12% pentoses, and 5% deoxyhexoses, in moles

(3) Excluding phospholipids, which have been included in (4)

(4) All phosphorus compounds, including both organic and inorganic compounds in the proportion given by Miyata and Hattori (1986)

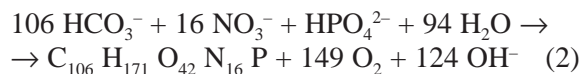
(5) Including tryptophan and 5.72% amidic -N

(6) Total chlorophylls with 56% chlorophyll *a*

(7) Proteins include chlorophylls in a ratio of chlorophyll *a*: protein nitrogen of 1.7 expressed as g Chl *a*: at N-Prt

(8) (Proteins + chlorophylls) + phosphorus compounds in the proportion needed for an atomic N:P ratio of 16:1

A C:N:P ratio = 106:16:1 and a  $Q_{CL}$  ratio = 0.79 yields a rounded elemental composition of  $C_{106}H_{171}O_{42}N_{16}P S_{0.3}Mg_{0.05}$ . This composition works out to a protein composition (including chlorophylls) of 47.4 %, a phosphorus compound composition of 12.0 %, a carbohydrate composition of 23.4 %, and a lipid composition of 17.2 % in weight, and, disregarding S and Mg, the overall equation for photosynthesis can be expressed as:



When the interest of a reaction lies in its stoichiometry, rather than its kinetics, and there are various ions in equilibrium, as in the case of the carbon dioxide or phosphate system, it is best to use the principal ion. For that reason, instead of fitting Equation 2 to  $CO_2$ , it is fit to the  $HCO_3^-$  ion, and hence the  $OH^-$  ion provides an approximate idea of changes in the pH during photosynthesis.

Using the  $O_2$  produced in Equation 2 yields a somewhat better Redfield ratio, namely,  $-O_2:C:N:P = 149:106:16:1$ . Calculating the ratio of each element to  $O_2$  separately is a very useful variation on this general relation and takes the form:

$$R_C = -\Delta O_2:\Delta C, R_N = -\Delta O_2:\Delta N \text{ and } R_P = -\Delta O_2:\Delta P \quad (3)$$

Based on Equation 2, the coefficient values are:  $R_C = 1.41$ ,  $R_N = 9.3$ , and  $R_P = 149$ . This value of  $R_C$  is consistent with the value published by Laws (1991), and the expression given above is practically identical to that given by Anderson (1995).

The numeric values for the Redfield ratio are

rather controversial (Sambroto *et al.*, 1993) and will continue to be so, and for that reason we always use the symbols  $R_C$ ,  $R_N$ , and  $R_P$  instead of their numeric values in the expressions to model anomalies in the Redfield stoichiometry. This means complicating the equations somewhat, but it allows each researcher to use the C:N:P and  $Q_{CL}$  ratio values he or she deems most appropriate. With these ratios, the equation can be used to calculate the values of  $R_C$ ,  $R_N$ , and  $R_P$  in a simple, direct manner (Fraga *et al.*, 1998):

$$R_C = (R_{CH} + (R_{CL} - R_{CH}) \cdot (1 + Q_{CL})) \cdot (1 - (C:N)_{PCP} / (C:N)) + R_{N(PCP)} / (C:N) \quad (4)$$

where  $R_{CH}$  and  $R_{CL}$  are the  $R_C$  values for carbohydrates and lipids, respectively;  $R_{N(PCP)}$  and  $(C:N)_{PCP}$  are the values of  $R_N$  and C:N for the overall protein + chlorophylls + phosphorus compounds overall. Taking these values from Table 2 gives:

$$R_C = (1.00 + 0.36 / (1 + Q_{CL})) \cdot (1 - 3.69 / (C:N)) + 5.81 / (C:N)$$

The other values are:  $R_N = R_C \cdot C:N$  and  $R_P = R_C \cdot C:P$ .

The value of  $R_C$  in Equation 4 depends on the C:N and  $Q_{CL}$  ratios and is not dependent on the N:P ratio because, as shown in Table 2, the values of  $R_C$  and  $R_N$  for the protein + chlorophyll together and the phosphorus compounds are practically the same.

## BROECKER'S TRACERS

The preformed nutrient concept originated by Redfield *et al.* (1963) can be used to detect and quantitatively assess anomalies occurring in phyto-

plankton photosynthesis in respect of general Equation 2:

$$\text{NO}_3^\circ = (\text{O}_2 - \text{O}_{2\text{sat}})/R_N + \text{NO}_3^- \quad (5)$$

where  $\text{NO}_3^\circ$  is the performed  $\text{NO}_3^-$  and  $\text{O}_{2\text{sat}}$  is saturated  $\text{O}_2$  at the winter formation temperature for the body of water in question; and the same follows for the other nutrients. Use of preformed nutrients is helpful in waters deeper than 200 m, where temperature can be viewed as a conservative property; but the preformed nutrient value is not conservative in the surface layer, where temperature varies as a result of the interchange of heat with the atmosphere.

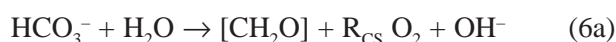
The preceding drawback can be overcome using Broecker's tracers (Broecker, 1974):

$$\begin{aligned} \text{"NO"} &= \text{O}_2 + R_N \cdot \text{NO}_3^-; \text{"PO"} = \text{O}_2 + R_P \cdot \text{PO}_4^{3-}; \\ \text{"CO"} &= \text{O}_2 + R_C \cdot \text{CO}_2 \end{aligned}$$

which are characteristic for every body of water and are independent of photosynthetic activity as long as the Redfield stoichiometry holds. Broecker's tracers vary according to the interchange of  $\text{O}_2$  with the atmosphere, but, as discussed later, this is not a shortcoming and can even be used to calculate the interchange itself.

### Synthesis when the Redfield stoichiometry does not hold

In the absence of nutrients, only carbohydrate synthesis,



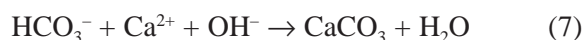
where  $R_{\text{CS}} = 1$ , or lipid synthesis, approximately



where  $R_{\text{CS}} = 1.36$ , is possible.

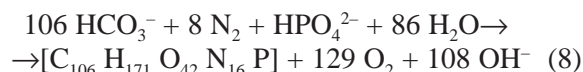
Therefore, both Equations 6a and 6b can be considered equivalent if the appropriate value of  $R_{\text{CS}}$  is used in each case (Ríos *et al.*, 1998).

Another important anomaly results from coccolithophore blooms, in which calcite is formed according to the equation



If nitrates have been depleted but phosphates are still available, cyanobacteria can still carry on biosynthe-

sis using the dissolved  $\text{N}_2$  in the water, according to the equation



Of the chemical Equations given above (Eqs. 2, 6a, 6b, 7 and 8), only Equation 2 satisfies the Redfield ratio. The others do not satisfy the ratio, and hence the values for Broecker's tracers "NO", "PO", and "CO" in these Equations are not constant. To be able to quantify all the above reactions, new tracers that remain constant are needed for use as reference values.

### Extension of the tracers

One tracer that does fulfil all the preceding equations (Eqs. 2, 6a, 6b, 7 and 8) could be:

$$\text{"XO"} = \text{O}_2 + c \text{CO}_2 + n \text{NO}_3 + p \text{PO}_4 + a \text{Ap} \quad (9)$$

and it therefore follows that

$$-\Delta\text{O}_2 = c \Delta\text{CO}_2 + n \Delta\text{NO}_3 + p \Delta\text{PO}_4 + a \Delta\text{Ap}$$

where Ap is potential alkalinity, being the sum of total alkalinity ( $A_T$ ) plus  $\text{NO}_3^-$ .  $A_p$  is not dependent on photosynthetic activity (Robertson *et al.*, 1994), and use of that value instead of  $A_T$  results in simpler tracers. In surface waters with potentially large quantities of ammonium and nitrite the Equation for potential alkalinity needs to be expanded to:

$$\text{Ap} = A_T + \text{NO}_3^- - \text{NH}_4^+ + 0.5 \text{NO}_2^- \quad (10)$$

For more details about the equation of Ap, see Annex I.

On the basis of the equalities (3) in Equation 2, the amount of  $\text{CO}_2$  consumed to form 1 mole of  $\text{O}_2$  is  $1/R_C$ ; for  $\text{NO}_3$  the value is  $1/R_N$  and for  $\text{PO}_4$  the value is  $1/R_P$ . There is no variation in potential alkalinity.

A similar reasoning applies to Equations 6-8. In Equation 8, 5/4 of the nitrogen used has to be subtracted from the  $\text{O}_2$  according to:



Table 3 presents this system of Equations in matrix form. The coefficient values for the different tracers in Equation 9 are obtained by taking the values of elements from one or more columns and from

TABLE 3. – Matrix of equations from those listed in the body of the text for calculating the coefficient values in Equation 9.

Equation	$\Delta\text{CO}_2$	$\Delta\text{NO}_3$	$\Delta\text{PO}_4$	$\Delta\text{A}_p$			$-\Delta\text{O}_2$
(2) Redfield	$1/R_C$	$1/R_N$	$1/R_P$	0	×	$\begin{vmatrix} c \\ n \\ p \\ a \end{vmatrix}$	$\begin{vmatrix} 1 \\ 1 \\ 0 \\ 1-5/(4 R_N) \end{vmatrix}$
(6) Carbohydrates. Lipids	$1/R_{CS}$	0	0	0			
(7) $\text{CaCO}_3$	1	0	0	2			
(8) $\text{N}_2$ fixation	$1/R_C$	0	$1/R_P$	0			
	A					B	C
	$B = A^{-1}C$						

$R_{CS} = 1$  for carbohydrates;  $R_{CS} = 1.36$  for lipids;  $R_C = 1.41$ ;  $R_N = 9.3$ ;  $R_P = 149$ .

TABLE 4. – Principal tracers used in calculating anomalies in Redfield stoichiometry (letters appearing in quotation marks {""} in the tracer nomenclature are the symbols for each of the chemical elements intervening in the calculation)

"NO" = $\text{O}_2 + R_N \cdot \text{NO}_3$
"PO" = $\text{O}_2 + R_P \cdot \text{PO}_4$
"CO" = $\text{O}_2 + R_C \cdot \text{CO}_2$
"CAO" = $\text{O}_2 + R_C(\text{CO}_2 - 0.5 \cdot \text{A}_p)$
"NCO" = $\text{O}_2 + R_{CS} \cdot \text{CO}_2 + (1 - R_{CS}/R_C)R_N \cdot \text{NO}_3$
"NPO" = $\text{O}_2 + \text{NO}_3 \cdot 5/4 + (1 - 5/(4 \cdot R_N))R_P \cdot \text{PO}_4$
"NCAO" = $\text{O}_2 + R_{CS}(\text{CO}_2 - 0.5 \cdot \text{A}_p) + (1 - R_{CS}/R_C)R_N \cdot \text{NO}_3$
"NPCO" = $\text{O}_2 + R_{CS} \cdot \text{CO}_2 + \text{NO}_3 \cdot 5/4 + (1 - R_{CS}/R_C - 5/(4 \cdot R_N))R_P \cdot \text{PO}_4$
"NPCAO" = $\text{O}_2 + R_{CS}(\text{CO}_2 - 0.5 \cdot \text{A}_p) + \text{NO}_3 \cdot 5/4 + (1 - R_{CS}/R_C - 5/(4 \cdot R_N))R_P \cdot \text{PO}_4$

where  $\text{O}_2$  and  $\text{NO}_3$  are the corrected values according to the following equations:

$$\begin{aligned} \text{O}_2 &= \text{O}_{2 \text{ obs}} - 0.5 \text{NO}_3^- - 2 \text{NH}_4^+ \\ \text{NO}_3 &= \text{NO}_3^- + \text{NO}_2^- + \text{NH}_4^+ \\ \text{A}_p &= \text{A}_T + \text{NO}_3^- - \text{NH}_4^+ + 0.5 \text{NO}_2^- \end{aligned}$$

$\text{A}_T$  = Total alkalinity.  $\text{A}_p$  = Potential alkalinity

the same number of rows in the matrix. Row 1 is always taken so that all the tracers are in accordance with the Redfield ratio.

The different matrix combinations yield a total of 15 tracer values. The tracer most useful in quantifying the most commonly occurring anomalies in the Redfield stoichiometry are summarized in Table 4.

Table 5 lists the conditions in which each of the tracer values is unchanged, marked by a black rectangle. Additionally, all the tracers exhibiting the same anomaly per mole of  $\text{C}_T$  used have been indexed using the same letter; differences in those anomalies will thus cancel out in the calculations. For those tracers that contain N but not P, the term  $R_N \cdot \text{NO}_3$  can be changed to  $R_P \cdot \text{PO}_4$  without any change in their properties.

As has already been mentioned, the principal anomalies are: *a*) accumulation or use of carbohydrates or lipids; *b*) precipitation of  $\text{CaCO}_3$ ; and *c*) fixing of  $\text{N}_2$ . All these anomalies can be quantified by combining the tracer satisfying the condition with another tracer that satisfies only the Redfield ratio. These tracer pairs could be "NCO" and "NO", "CAO" and "CO", and "NPO" and "PO". The most

TABLE 5. – Variations in the tracers for the different reactions; ■ indicates reactions in which the tracer remains constant; identical letters indicate reactions in which tracers vary in the same amount

	$\Delta\text{O}_2$	$\Delta\text{CO}_2$	Cbh	$\text{N}_2$	$\text{CaCO}_3$	Red.
"NO"	d	■	g	i	■	■
"PO"	d	■	g	-j	■	■
"CO"	d	e	-h	-j	-l	■
"CAO"	d	e	-h	k	■	■
"NCO"	d	f	■	k	-m	■
"NPO"	d	■	h	■	■	■
"NCAO"	d	f	■	k	■	■
"NPCO"	d	f	■	■	-m	■
"NPCAO"	d	f	■	■	■	■

$\Delta\text{O}_2$  and  $\Delta\text{CO}_2$ : Interchange with the atmosphere  
 Cbh: Synthesis or use of carbohydrates or lipids  
 $\text{N}_2$ : Cyanophycean  $\text{N}_2$  fixation  
 $\text{CaCO}_3$ : Coccolithophores or precipitation and dissolution of  $\text{CaCO}_3$   
 Red: Biomass synthesis or mineralization according to Redfield stoichiometry

complex case that can occur is a mix of different phytoplanktonic populations giving rise to all three anomalies *a*, *b*, and *c* simultaneously. For this case the tracer "NPCAO" satisfies all three anomalies, whereas the tracers "NPO", "NPCO", and "NCAO" each fail to satisfy one, namely, *a*, *b*, or *c*, respectively. Using each of those tracers separately in conjunction with "NPCAO" enables each of the anomalies to be quantified individually within the system as a whole.

Thus, all the tracers that contain C are affected by the interchange of  $\text{CO}_2$  with the atmosphere. Nevertheless, in most cases the interchange can be disregarded, because there is a tendency towards compensation. Solar radiation in the surface layer gives rise to photosynthesis, leading to a  $\text{CO}_2$  deficit while at the same time raising the water temperature, thereby blocking inputs of  $\text{CO}_2$  from the atmosphere. The decrease in  $\text{CO}_2$  pressure ( $p\text{CO}_2$ ) of 10  $\mu\text{moles/kg}$  of organic carbon brought about by photosynthesis is offset by a temperature increase of 1.3°C. In coccolithophore populations calcite plate formation also reduces the decrease in  $p\text{CO}_2$  brought

about by photosynthesis. For a calcification ratio of 1, the decrease in pressure is only 32% of the level that would attain without precipitation of  $\text{CaCO}_3$ , and a temperature increase of only  $0.54^\circ\text{C}$  per 10  $\mu\text{moles/kg}$  of organic carbon synthesized suffices to offset any change in  $\text{pCO}_2$ . Furthermore, the slow rate of  $\text{CO}_2$  interchange means that over an interval of days, values can be considered constant.

#### PHYTOPLANKTON STRATEGIES INVOLVING SYNTHESIS THAT DOES NOT SATISFY THE REDFIELD RATIO

This category includes groups of phytoplankton that employ different strategies to obtain one or more nutrients that have been depleted in the photic layer to enable continued growth. This category also includes diatoms, which give rise to alterations in the Redfield ratio when nutrients are depleted in the photic zone, even though they do not have a strategy for continued growth.

#### End of a diatom bloom

In the presence of sufficient nutrients and light, diatoms divide exponentially, consuming nutrients until they have been depleted, thereby limiting maximum biomass production. Nutrient-poor conditions prevent diatoms from dividing further, but their photosynthesizing apparatus continues to produce even more carbohydrates than they are able to store, and the excess is released into the environment in soluble form (Goldman *et al.*, 1992). Finally, the population dissipates as a result of sedimentation and predation. Therefore, at the biomass peak during the bloom, photosynthesis no longer follows Equation 2 but instead follows Equation 6a, thereby deviating from the Redfield ratio. The value of "NO" increases, because of  $\text{O}_2$  production that is not offset by  $\text{NO}_3$  consumption; and the value of "CO" decreases, because  $\text{O}_2$  production is only 1 mole per mole of  $\text{CO}_2$  consumed instead of 1.41 moles, while the value of "NCO" remains unchanged (Table 5).

The anomalies in these tracers are graphically represented in Figure 1, where  $Z_1$  is the depth of the nutrient-depleted zone and  $Z_D$  is the depth at which there are no longer any anomalies due to biological activity.

"NCO" is a conservative tracer, while "NO" ceases to be conservative and increases with carbohydrate synthesis, hence the amount synthesized in the photic zone can be calculated quantitatively

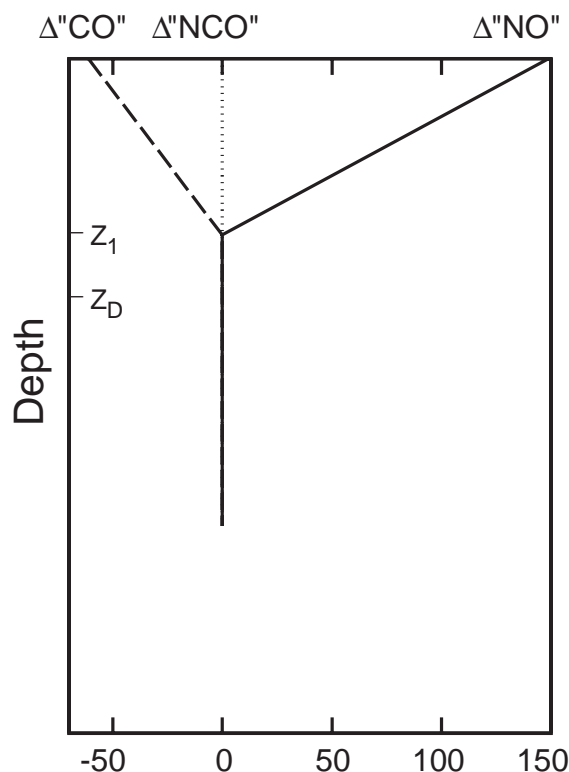


FIG. 1. – Theoretical plot of anomalies in "NO" and "CO" produced by excess carbohydrate synthesis, also plotting the conservative tracer "NCO".  $Z_1$  is the depth of the region of nutrient depletion;  $Z_D$  is the depth at which there are no more anomalies.

using the equation:

$$\text{C-Cbh} = \Delta$$
"NO" –  $\Delta$ "NCO" (11)

Broecker's tracers are all in units of  $\text{O}_2$ , but bearing in mind Equation 6a, one mole of carbohydrate carbon is produced for every mole of  $\text{O}_2$ . Accordingly, the result can be expressed either as moles of  $\text{O}_2$  or moles of C-Cbh.

Because anomalies in "NO" are opposed to anomalies in "CO", the following Equation can also be used:

$$\text{C-Cbh} = (\Delta$$
"NO" –  $\Delta$ "CO")/ $R_C$  (12)

in which division by  $R_C$  is performed to convert from moles of  $\text{O}_2$  to moles of carbon.

In both Equations 11 and 12  $\Delta$ "NO" = "NO" – "NO"<sub>D</sub> and  $\Delta$ "NCO" = "NCO" – "NCO"<sub>D</sub>, where "NO"<sub>D</sub> and "NCO"<sub>D</sub> are "NO" and "NCO", respectively, at the reference depth  $Z_D$  (Fig. 1).

The preceding equations are used to calculate the total carbohydrate value, which includes the carbohydrates stored within each cell plus those released into the environment as exudate.

Maximum biomass, expressed as carbon, which may be carbon synthesized in keeping with the Redfield ratio, is a function of the available nitrogen in the photic zone. Assuming that to be the same as the amount present in the water at depth  $Z_D$  taken as the reference value ( $\text{NO}_{3D}$ ), it then follows that:

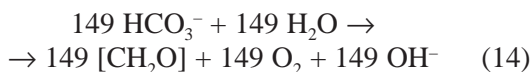
$$\text{C-Red} = (\text{NO}_{3D} - \text{NO}_3) \cdot R_N/R_C \quad (13)$$

where C-Red is moles of carbon and  $\text{NO}_3$  is unconsumed nitrate, in this case zero. This makes it possible to calculate the relative importance of carbohydrate synthesis vs. biomass production consistent with the Redfield ratio. The value of  $\text{C-Cbh}/(\text{C-Cbh} + \text{C-Red})$  can reach 28%.

### Vertically migrating dinoflagellates

As mentioned above in the Introduction, certain dinoflagellates that are able to carry out vertical migrations may synthesize carbohydrates in the nutrient-poor photic zone during the daytime. These carbohydrates are then stored within the cell. At dusk the dinoflagellates then descend to the subphotic zone, which is rich in nutrients, where they synthesize proteins and nucleic acids using the stored carbohydrate reserves. At daybreak the dinoflagellates return to the photic zone to begin a fresh cycle (Cullen, 1985; Cullen *et al.*, 1985). This is represented by the following Equations (Fraga *et al.*, 1992, 1999):

Photic zone:



Subphotic zone:

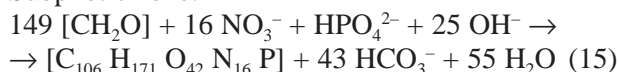


Figure 2 graphically represents the theoretical variations in the tracers "NO", "CO", and "NCO" calculated using Equations 14 and 15.  $Z_C$  is the depth at which carbohydrate synthesis is in equilibrium with carbohydrate use, and  $Z_D$  is the depth at which phytoplankton activity no longer produces anomalies in the tracer values. The term photic zone as used here is the water layer from 0 m to  $Z_C$ , and the subphotic zone is the layer from  $Z_C$  to  $Z_D$ . Figure 2 also shows the effect of losses of  $\text{O}_2$  to the atmosphere, shifting all the tracer values towards lower levels; that effect tapers off with depth.

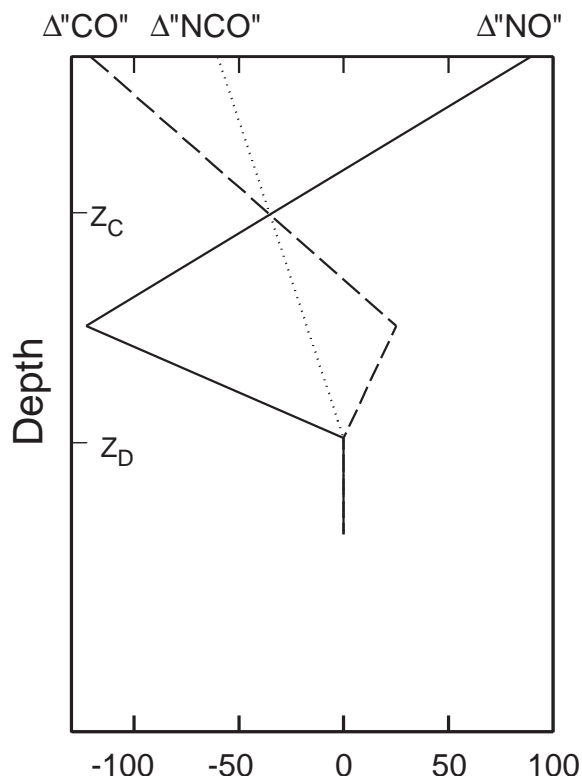


FIG. 2. – Theoretical plot of "NO" and "CO" anomalies according to equations (14) and (15) produced by migratory dinoflagellates, also plotting the effect of losses of  $\text{O}_2$  to the atmosphere.

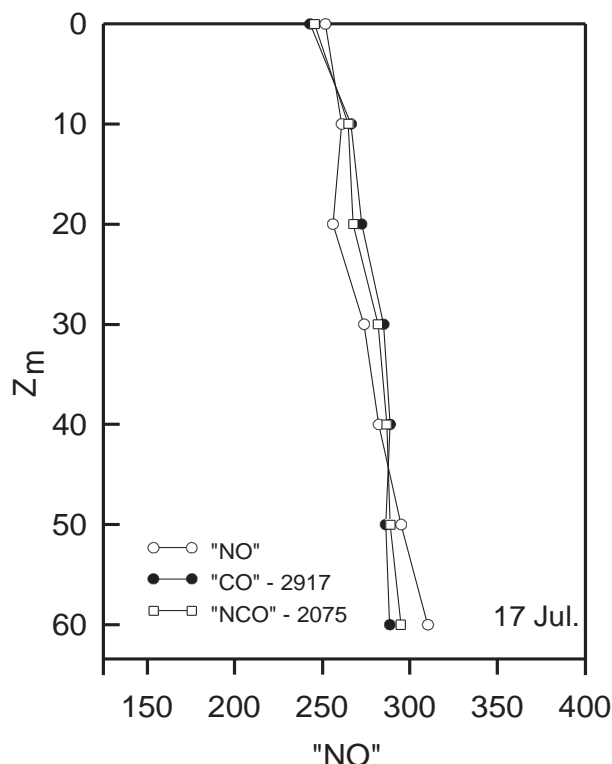


FIG. 3. – Distribution of "NO", "CO", and "NCO" during a period of upwelling (17 July). An amount of 2917 ( $= R_C \cdot \text{CO}_2^0 - R_N \cdot \text{NO}_3^0$ ) has been subtracted from "CO" and  $2917/R_C$  has been subtracted from "NCO" so that the scales for those tracers will coincide with that for "NO".

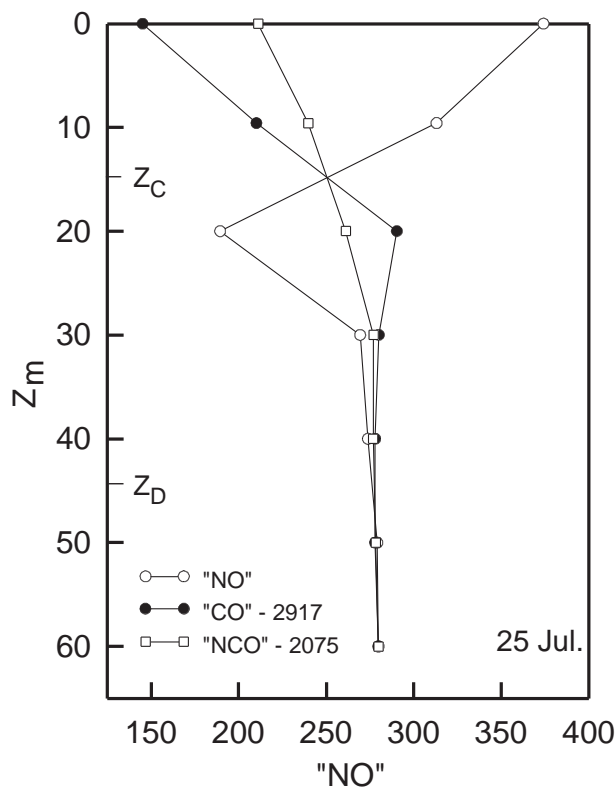


FIG. 4. – The same plot as in Figure 2 eight days later after a relaxation of upwelling (25 July) and occurrence of a red tide bloom.

Upwelling regions with variable upwelling activity are the best zones for observing the anomalies produced by this strategy on the part of migratory dinoflagellates. In conditions of active upwelling, nutrients are carried to the surface, and photosynthesis follows the Redfield ratio. Consequently, the vertical profiles for the three tracers take the form of straight lines, which may overlap. When upwelling intensity has abated and the nutrients in the photic zone have become depleted, migratory dinoflagellates gain the advantage, and the anomalies shown in the diagram in Figure 2 occur. The area off the northwestern Iberian Peninsula is one such zone, where intense upwelling interspersed with relaxation periods takes place in spring-summer (Álvarez-Salgado *et al.*, 1993). Figure 3 depicts the vertical profiles for the tracers “NO”, “CO”, and “NCO” during an episode of upwelling that carried nitrates up to the surface (17 July), and Figure 4 presents those same profiles at the same geographic location after a week of lower upwelling activity (25 July), with depletion of nutrients down to 20 m. Figure 5 plots the  $\text{NO}_3$ ,  $\text{CO}_2$ , and  $\text{O}_2$  distributions, clearly showing the vertical decoupling between  $\text{NO}_3$  and

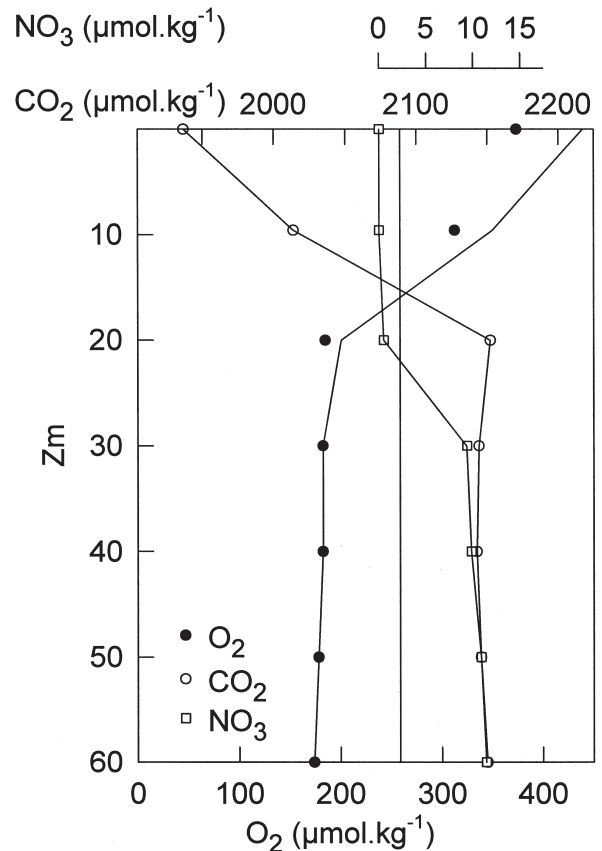


FIG. 5. – Vertical distribution of  $\text{O}_2$ ,  $\text{CO}_2$ , and  $\text{NO}_3$  at the station in Figure 4 on 25 July. The relative magnitude of each of the units is proportional to inverse Redfield stoichiometry. The preformed  $\text{CO}_2$  and  $\text{NO}_3$  values and  $\text{O}_2$  saturation at  $Z_D$  have been adjusted to the vertical line in the centre of the Figure. Solid data points are real  $\text{O}_2$  values; solid line represents the values adjusted for losses of  $\text{O}_2$  to the atmosphere.

$\text{CO}_2$  giving rise to the anomalies in “NO” and “CO” in Figure 4. The dominant species was the ciliate *Mesodinium rubrum*, whose behavioural pattern is identical to that of migratory dinoflagellates.

Equations 11 and 12 described above are applicable both to carbohydrate synthesis and usage. These equations give total values, calculated on a cumulative basis for all days elapsed since the start of nutrient depletion (in this case, six days), independently of whether the carbohydrates are used in the subphotic layer daily, and they are not dependent on losses of  $\text{O}_2$  to the atmosphere, because such losses affect all three tracers equally.

The relative importance of this biomass synthesis strategy compared to the usual pathway (Eq. 2) can be calculated as already described above. Accordingly, at the same station referred to above on 25 July (Fig. 4), integration from 0 m to  $Z_C$  yields a synthesis value of 987 mmoles of carbohydrate carbon/m<sup>2</sup>. Since nitrate at depth  $Z_D$  was 8  $\mu\text{moles/kg}$ ,



the biomass synthesized according to the Redfield ratio, also integrated from 0 m to  $Z_C$  (15 m), was 817 mmol/m<sup>2</sup>, for a total of 1 804 mmol/m<sup>2</sup>; that is, 55 % of the carbon was fixed by the carbohydrate pathway and 45% by the normal pathway of Equation 2. The example considered is for peak production by *M. rubrum*, but even so, the mean value was around 35 % at the locality in question during the period of upwelling relaxation that followed, and hence it is an important pathway for biomass synthesis.

Unlike the final stage of a diatom bloom, in which an amount of soluble carbohydrate remained, the final product here is biomass in accordance with Redfield's C:N ratio. Adding Equation 14 to Equation 15 yields Equation 2, which satisfies the Redfield ratio; thus, even though the ratio is not satisfied in either the photic zone or the subphotic zone, the total of the two zones combined does satisfy the ratio. This is because the carbohydrates synthesized in the photic zone are not a final product but rather a raw material input for the biosynthesis of proteins and nucleic acids in the subphotic zone.

### Losses of O<sub>2</sub> to the atmosphere

This section has been included because it is closely related to excess carbohydrate synthesis.  $\text{NO}_3 \cdot R_N$  is the maximum quantity of O<sub>2</sub> that can be produced beyond the saturation point, provided that the Redfield ratio is satisfied, and even taking into account the rise in surface temperature, it is likely that O<sub>2</sub> supersaturation is not much greater than 120%. As already mentioned, even after depletion of nutrients at the surface, certain dinoflagellates are able to continue to carry out photosynthesis and to produce O<sub>2</sub>, the only constraint being their ability to perform vertical migrations. O<sub>2</sub> saturation levels of up to 158% have been measured in these zones. As a consequence, the zones where the greatest losses of O<sub>2</sub> occur are those in which the Redfield ratio is not satisfied. The tracer "NO", sometimes used for this purpose, is only conservative if the Redfield ratio is satisfied, and therefore it should not be used to calculate losses of O<sub>2</sub>, particularly when nitrate levels in the surface waters are less than 0.5 μmol/kg. Figure 4 clearly shows that the higher the level of carbohydrate synthesis, and hence O<sub>2</sub> production, the higher the value of "NO". Paradoxically, at high losses of O<sub>2</sub>, the value calculated using "NO" yields inputs from, rather than losses to, the atmosphere.

When dinoflagellates are present, the "NCO" tracer has to be used. Oxygen losses, O<sub>2L</sub>, are:

$$O_{2L} = \Delta \text{"NCO"} \text{ where } \Delta \text{"NCO"} = \text{"NCO"} - \text{"NCO"}_D$$

A negative O<sub>2L</sub> value reflects losses of O<sub>2</sub> to the atmosphere. When coccolithophores or cyanobacteria are present, the corresponding conservative tracer for the species group present should be used instead of "NCO" (Table 5).

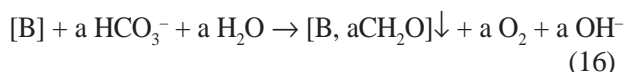
### Strategy of Rhizosolenia

The strategy employed by *Rhizosolenia* and other large diatoms is very similar to that of dinoflagellates, except that proteins and nucleic acids are not synthesized from carbohydrates in the subphotic layer. According to Villareal *et al.* (1993), *Rhizosolenia* takes up nitrates (and presumably phosphate as well) in the subphotic zone and transports them to the photic zone, where biomass is photosynthesized.

Although there are insufficient data to enable preparation of a definitive flow diagram for the stoichiometric processes, certain possibilities can nonetheless be put forward. To that end, live cell biomass has been designated B, with a mean composition of B = [C<sub>106</sub> H<sub>171</sub> O<sub>42</sub> N<sub>16</sub> P]. For ease of comprehension, substances accumulated inside the cell and transported vertically from one zone to the other have been placed in brackets [ ], with an arrow to the right of the brackets indicating the direction of vertical migration of the cells.

#### Photic zone

Initially there is excess carbohydrate synthesis, which provides cells with energy reserves and is also conducive to sinking of cells (Richard and Cullen 1995):

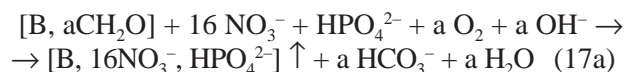


The amount of carbohydrates synthesized has been designated "a", because there is no theoretical relationship with the nutrients used.

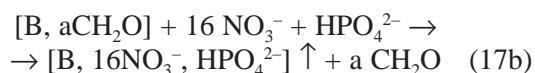
#### Subphotic zone

Nutrients in this layer are taken up into the interior of the cells, resulting in carbohydrate oxidation by respiration, which in turn could supply the ener-

gy needed to drive concentration of the nutrients present in the water at the  $\mu\text{mole/l}$  level, from where they are taken up into the cell plasma attaining a concentration on the order of  $\text{mmoles/l}$ , that is, some thousand times greater. The Equation for this is:



On the other hand, release of soluble carbohydrates into the sea to allow the cells to rise to the surface is also a possibility, according to the equation:

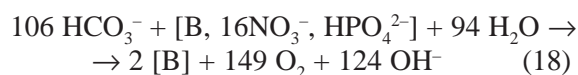


This latter possibility would seem to be unlikely, because living organisms tend to optimize utilization of their energy reserves.

In both cases, i.e. Equations 17a and 17b, cells with their stores of nitrates (Villareal *et al.*, 1996) and phosphates float back to the photic zone.

### Photic zone

In the photic zone the cells containing the transported nutrients photosynthesize biomass according to the Equation:



Therefore, two stages of the process, namely, those represented by Equations 16 and 18, take place in the photic zone. Taken together, this gives:

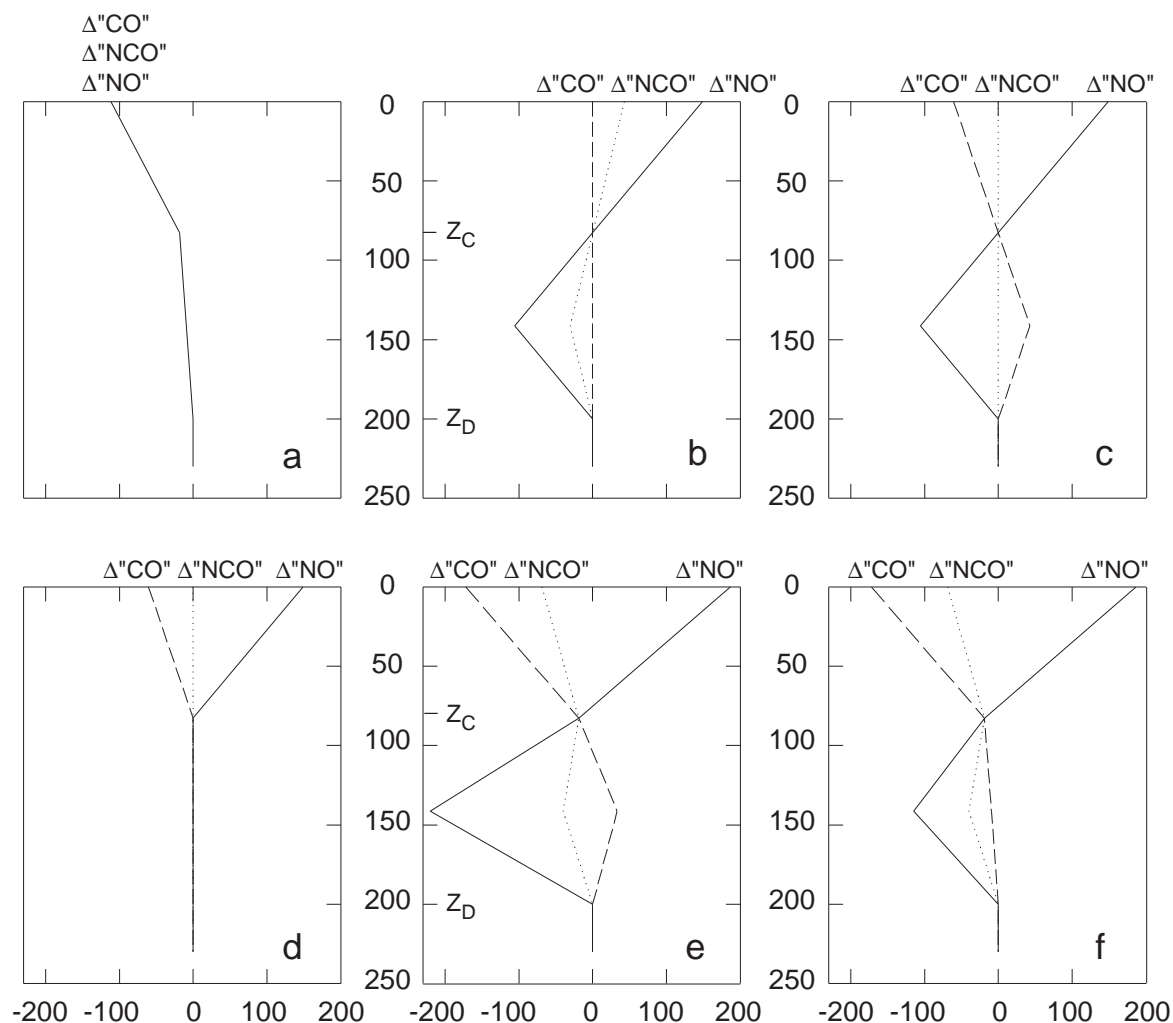
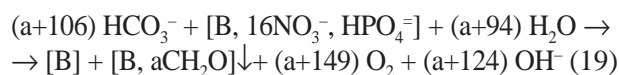


FIG. 6. – Changes in the tracers “NO”, “CO”, and “NCO” caused by different processes: a) losses of  $\text{O}_2$  to the atmosphere; b) transport of  $\text{NO}_3^-$  from the subphotic zone to the photic zone; c) carbohydrate synthesis in the photic zone for conversion in the subphotic zone; d) as in c) but carbohydrates are lost as exudate in the subphotic zone; e) sum of processes a+b+c; f) sum of processes a+b+d.

The anomalies in the tracers “NO”, “CO”, and “NCO” occurring in these two processes, namely, carbohydrate synthesis and transport of  $\text{NO}_3^-$  ions, have been graphically represented separately (Fig. 6), and additionally another anomaly has been shown, namely, the anomaly resulting from losses of  $\text{O}_2$  to the atmosphere (Fig. 6a). The decrease in the values of these tracers brought about by the loss of  $\text{O}_2$  is the same for all the tracers, hence the differences between the tracers are independent of losses of  $\text{O}_2$ .

During transport of the  $\text{NO}_3^-$  ions from the subphotic zone to the photic zone (Figure 6b), the tracer “NCO” ceases to be conservative, and the anomaly in this tracer is proportional to the transport of  $\text{NO}_3^-$  and is independent of carbohydrate synthesis (Figs. 6c, 6d).

Figures 6c and 6d depict the anomalies brought about by carbohydrate synthesis in the photic zone (Eq. 16). In the subphotic zone (Fig. 6c) anomalies occur as a result of the use of carbohydrates in respiration (Eq. 17a), while Figure 6d depicts the case in which carbohydrates are released by the cells to the exterior in soluble form (Eq. 17b). The final outcome is the total of all the anomalies brought about by all three processes, as shown in Figures 6a + 6b + 6c and summarized in Figure 6e, or as shown in Figures 6a + 6b + 6d and summarized in Figure 6f.

The presence of an “NO” minimum in the subphotic zone in Figures 6e and 6f agrees with the data published by Emerson and Hayward (1995), who found that when the nutricline in a subtropical region in the North Pacific was below the 1% light level, preformed nitrate ( $\text{NO}_3^0$ ) was negative, with a minimum at around 140 m. The presence of an “NO” minimum can also be inferred from the relation “NO” =  $\text{O}_{2\text{sat}} + R_N \cdot \text{NO}_3^0$ .

As already mentioned above, the tracer “NCO” is not conservative when  $\text{NO}_3^-$  transport occurs, but there are two levels,  $Z_C$  and  $Z_D$ , where it does not undergo any alteration. Interpolation of the “NCO” values between  $Z_C$  and  $Z_D$  yields a series of undisturbed values that can be taken as benchmarks for calculating the anomalies. Designating this series of reference values “NCO”<sub>r</sub>, the quantity of  $\text{NO}_3^-$  transported from each level of the subphotic zone to the photic zone is:

$$T_{(\text{NO}_3^-)} = (\Delta''\text{NCO}''_r - \Delta''\text{NCO}'') / (R_N \cdot (1 - 1/R_C)) \quad (20)$$

where  $T_{(\text{NO}_3^-)}$  is transported nitrate expressed as  $\text{NO}_3^-$  (moles/kg), and the quantity of carbohydrates used at each level of the subphotic zone is:

$$\text{C-Cbh} = (\Delta''\text{CO}'' - \Delta''\text{NCO}''_r) / (R_C - 1)$$

expressed as carbon (moles/kg).

In the photic zone the sum of synthesized carbohydrates plus organic carbon synthesized from the imported nitrate is given by the relation:

$$\text{C-Cbh} + T_{(\text{NO}_3^-)} \cdot R_N / R_C = (\Delta''\text{NO}'' - \Delta''\text{CO}'') / R_C$$

where  $T_{(\text{NO}_3^-)}$ , expressed as moles/kg of nitrogen (Eq. 20), is converted to carbon by multiplying it by the factor  $R_N/R_C$ .

While this is true for each layer separately, the values of C-Cbh and  $T_{(\text{NO}_3^-)}$  cannot be calculated independently of each other, because biomass synthesis and carbohydrate synthesis may be vertically decoupled in the photic zone, for which there are no benchmark “NCO”<sub>r</sub> reference values. Carbohydrate synthesis can be calculated globally for the entire photic zone as a whole by integrating from 0 m to  $Z_C$ .

$$\text{C-Cbh} = (\Delta''\text{NO}'' - \Delta''\text{CO}'' - T_{(\text{NO}_3^-)} \cdot R_N) / R_C$$

$T_{(\text{NO}_3^-)}$  here being the total nitrate imported from the subphotic zone, all values being expressed as moles/m<sup>2</sup>.

The previous schemes did not take into account the input of  $\text{CO}_2$  from the atmosphere to compensate consumption during photosynthesis. *Rhizosolenia* occurs during periods of prolonged stability; under these conditions, the exchange of gases can be large, not only by  $\text{O}_2$  losses, but also due to  $\text{CO}_2$  inputs; therefore, the signature produced by carbohydrate synthesis in the upper water layers may be fairly weak.

Despite these limitations, anomalies in the tracers “NCO”, “NO”, and “CO” can still provide very clear quantitative information as to what has been happening from the surface down to the level below the nutricline.

## Coccolithophores

According to Buitenhuis *et al.* (1999), coccolithophores can synthesize calcite from the  $\text{HCO}_3^-$  ion. This provides a supply of  $\text{CO}_2$  without their having to expend energy on concentrating the dissolved free  $\text{CO}_2$ , based on the following intracellular reactions:

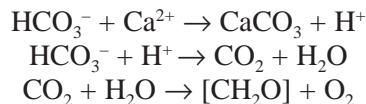


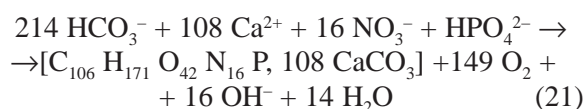
TABLE 6. – Changes in the concentration of the principal ions in the CO<sub>2</sub> system in the formation of 106 μmol/kg of organic carbon during photosynthesis by coccolithophores (calculations have assumed that Ca<sup>2+</sup><sub>in</sub>·CO<sub>3</sub><sup>2-</sup><sub>in</sub> = Ca<sup>2+</sup><sub>fin</sub>·CO<sub>3</sub><sup>2-</sup><sub>fin</sub>)

Ion	Initial value	Final	Final value	Δ: Final – Initial
C <sub>T</sub>	2077*	C <sub>T,fin</sub> – 106 – CaCO <sub>3,fin</sub> =	1863.0	-213.9
A	2317*	A <sub>in</sub> + 106·R <sub>C</sub> /R <sub>N</sub> – 2·CaCO <sub>3,fin</sub> =	2117.2	-199.8
Ca <sup>2+</sup>	10300.9*	Ca <sup>2+</sup> <sub>in</sub> – CaCO <sub>3,fin</sub> =	10193.0	-107.9
H <sub>2</sub> CO <sub>3</sub>	13.7		10.7	-3.0
HCO <sub>3</sub> <sup>-</sup>	1895.4		1682.8	-212.7
CO <sub>3</sub> <sup>2-</sup>	167.8	CO <sub>3</sub> <sup>2-</sup> <sub>in</sub> · Ca <sup>2+</sup> <sub>in</sub> / (Ca <sup>2+</sup> <sub>in</sub> – CaCO <sub>3,fin</sub> ) =	169.6	1.8
CaCO <sub>3</sub>	0	CaCO <sub>3,fin</sub> =	107.9	107.9

Literature values have been marked with an asterisk (\*); all other values have been calculated using the CO<sub>2</sub> system dissociation constants S = 35; t = 15; C<sub>T</sub> = total carbon; A = alkalinity; CaCO<sub>3</sub> from coccoliths

where the H<sup>+</sup> produced during the formation of CaCO<sub>3</sub> releases one mole of CO<sub>2</sub>, which is used to synthesize organic carbon. Thus, the calcification reaction ΔCaCO<sub>3</sub>/ΔCorg is equal to 1.

Another approach is to consider maximum energy usage in the framework of the CaCO<sub>3</sub> precipitation-dissolution balance when the system is in chemical equilibrium. Table 6 presents the variations in each ion while the ionic product of calcium carbonate is held constant, CO<sub>3</sub><sup>2-</sup> × Ca<sup>2+</sup> = const. The “initial value” column gives the characteristic values for biologically undisturbed sea water, and the column setting out the “final” values give the final value and variation for each ion during synthesis of 106 μmoles/kg of organic carbon for coccolithophore biomass formation. Column Δ shows that the variations in the ΔH<sub>2</sub>CO<sub>3</sub> (free CO<sub>2</sub> dissolved in the water) and ΔCO<sub>3</sub><sup>2-</sup> are small and opposite, and their difference can be included in the value of ΔHCO<sub>3</sub><sup>-</sup>. The resulting values can be used to construct a simplified stoichiometric equation:



The calcification ratio is 1.02, practically the same as the previous value and slightly closer to the value of 1.07 reported by Paasche (1998) for cultures incubated in nutrient-sufficient conditions.

However, this Equation is not practical, because the calcification ratio can vary considerably, from 0.2 (Holligan *et al.*, 1993) to 1.4 (Paasche, 1998). The highest calcification ratios have been observed in cultures grown in nutrient-poor conditions. For that reason, calcium carbonate formation (Eq. 7) and synthesis of organic matter have been considered separately in the Equations in Table 3. Thus, the tracer values used are suitable for all calcification ratios and even for variations caused by the dissolu-

tion or precipitation of CaCO<sub>3</sub> of chemical origin without any involvement by coccolithophores. The preceding Equation can, accordingly, be considered the sum of Equation 2, which satisfies Redfield stoichiometry, and Equation 7 multiplied by 108.

Besides CaCO<sub>3</sub>, coccolithophores also store accumulations of lipids as energy reserves, in addition to the structural lipids present in all phytoplanktonic cells. Based on the biochemical composition of *Emiliana huxleyi* reported by Fernández *et al.* (1994), the reserves would appear to comprise 12% carbohydrates and 88% lipids, yielding R<sub>CS</sub> = 1.3.

Therefore, “NCAO” has to be used as the conservative tracer. This tracer is not dependent on CaCO<sub>3</sub> formation or lipid accumulation. The tracers “NCO” and “NO”, the former being invariable with excess lipid synthesis and variable with CaCO<sub>3</sub> formation and the latter (“NO”) being the converse. This enables the values for CaCO<sub>3</sub> and excess lipid formation to be calculated separately. The respective Equations, expressed as number of carbon atoms, are:

$$\text{CaCO}_3 = (\Delta\text{“NCAO”} - \Delta\text{“NCO”})/R_{CS} \quad (22) \\ \text{C-Lipids} = (\Delta\text{“NO”} - \Delta\text{“NCAO”})/R_{CS}$$

or

$$\text{CaCO}_3 = -\Delta\text{Ap}/2 \\ \text{C-Lipids} = (\Delta\text{“NO”} - \Delta\text{“CAO”})/R_C$$

The plot in Figure 7 illustrates the anomalies in the tracers “NO” and “NCO” as well as in the conservative tracer “NCAO”, in which both photosynthesis and coccolithophore plate formation take place in the upper layer of the water column. The plot is only an approximation because the calcification:photosynthesis ratio is variable (Marañón and González, 1997). Accordingly, “NCO” and “NO” are independent, and the anomalies in those tracers need not follow any fixed pattern. If coccoliths drift down into the subphotic zone from the upper levels and dissolve there, the “NCO” value could increase.

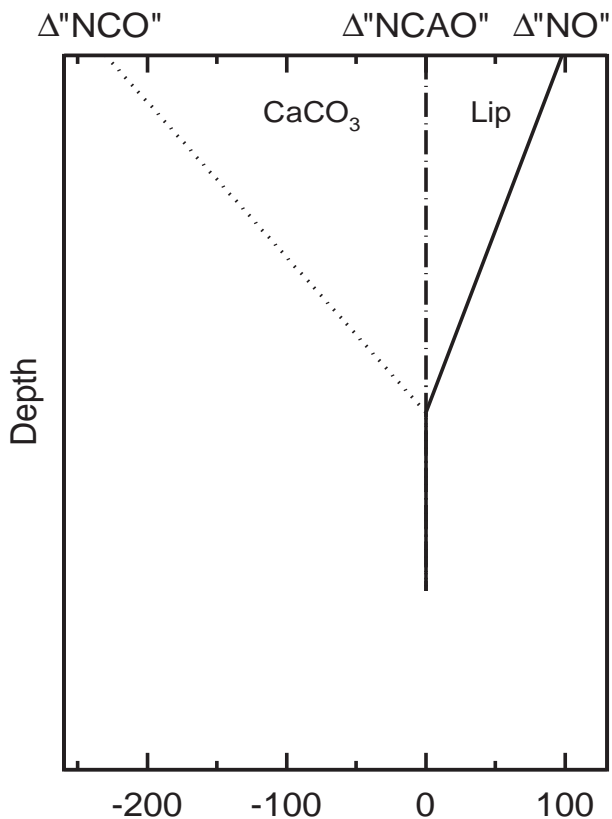


FIG. 7. – Theoretical plot of changes in the tracers “NCO” and “NO” during a coccolithophore bloom, assuming both calcite ( $\text{CaCO}_3$ ) scale formation and accumulation of lipids in the cells.

Experimental methodology is a question of great significance in the study of coccolithophores, since when they are present modifications are often required, something usually unnecessary on normal oceanographic cruises. When direct measurements of total  $\text{CO}_2$  and alkalinity are taken in the presence of coccoliths, samples need to be filtered (Robertson *et al.*, 1994), because at pH 5.2–5.5 coccoliths dissolve in fewer than 30 seconds (Balch *et al.*, 1996), thereby producing erroneously high alkalinity and total  $\text{CO}_2$  readings.

The difference in the alkalinity values for a filtered sample and an unfiltered sample will give the amount of  $\text{CaCO}_3$  present in the samples. Subtracting the value calculated using Equation 22 from that  $\text{CaCO}_3$  value yields the amount that has sedimented out of the water layer concerned, if the value is positive, or the amount that has entered that layer from higher levels, if the value is negative.

The plot in Figure 7 has disregarded possible reactions in the water level below, but in addition to the dissolution of coccoliths already referred to above, coccolithophores might also employ a strategy analogous to that of dinoflagellates that are able to carry out vertical migrations. Support for this pos-

sibility comes from the finding that when nutrients in the photic zone become scarce, coccolithophores store lipids, which can then be used to synthesize proteins in darkness (Fernández *et al.*, 1994). In addition, coccolith formation increases in nutrient-poor conditions (Paasche, 1998), resulting in an increase in density conducive to sinking. The cells may be able to return to the photic zone by releasing their calcite plates. This has not been demonstrated, however; and, indeed, coccolithophore cultures carried out in conditions of low light levels have shown that coccolith formation continues, though at a slower rate (Balch *et al.*, 1996). Correct use of Broecker’s tracers could thus be a good way to elucidate coccolithophore behaviour in the wild.

### $\text{N}_2$ fixing

If the values for “NO”, “PO”, and “CO” are known, the nutrient limiting biological production is the one with the lowest value. “CO” is of course always much higher than the other two, because the rate of  $\text{CO}_2$  usage is 9.6 times higher than  $\text{NO}_3^-$  and  $\text{PO}_4^-$  (Redfield *et al.*, 1963). The values of “NO” and “PO” are usually the same, because  $\text{NO}_3^-$  and  $\text{PO}_4^-$  are depleted together. When the nutrients  $\text{NO}_3^- + \text{NO}_2^- + \text{NH}_4^+$  are depleted in the photic zone but  $\text{PO}_4^-$  is still available, “NO” < “PO”, and in those conditions cyanobacteria gain the advantage and begin fixing  $\text{N}_2$  according to Equation 8.

“NPO” can be used as the conservative tracer until the phosphate is depleted. Figure 8 presents a theoretical plot of what takes place during  $\text{N}_2$  fixation in the surface layer. Water with “NO” < “PO” from level  $Z_D$  disseminates towards the surface. Biomass production takes place through photosynthesis in the photic zone with consumption of  $\text{PO}_4^-$  and production of  $\text{O}_2$ . According to Equation 8,  $\text{O}_2$  production per atom of P is 129 rather than 149 (Eq. 2), hence “PO” decreases. In its turn,  $\text{O}_2$  production is carried on without  $\text{NO}_3^-$  consumption, and hence “NO” increases until the  $\text{PO}_4^-$  has been depleted, making the values of the tracers “NO” and “PO” equal. From that point, mineralization of the biomass formed commences in accordance with Redfield stoichiometry, and thus there is no further change to the values. For the sake of simplicity losses of  $\text{O}_2$  to the atmosphere have been left out of Figure 8, whereby “NPO” remains invariable. In reality  $\text{O}_2$  losses are usually large, and the three tracers are shifted towards lower values at the surface, though the differences among them persist at all times.

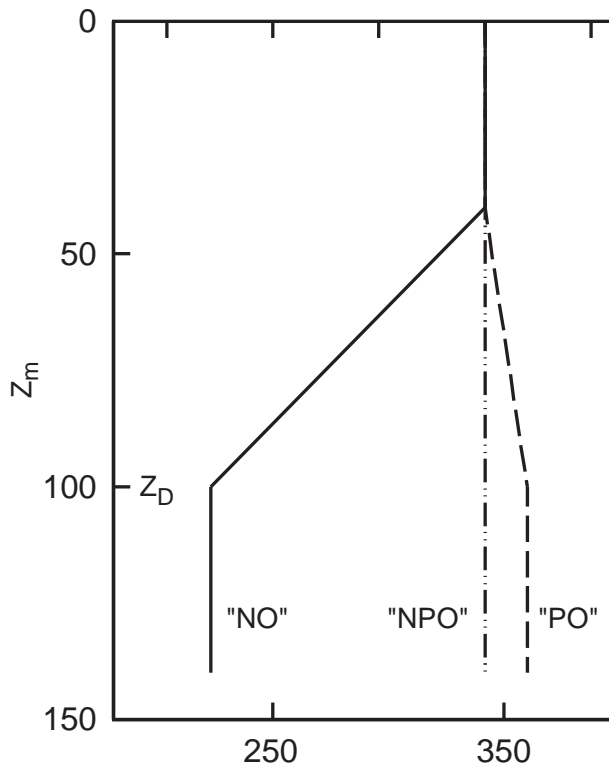


FIG. 8. – Theoretical plot of changes in the tracers “NO” and “PO” caused by  $N_2$  fixation by a cyanophycean population in nitrate-depleted water.

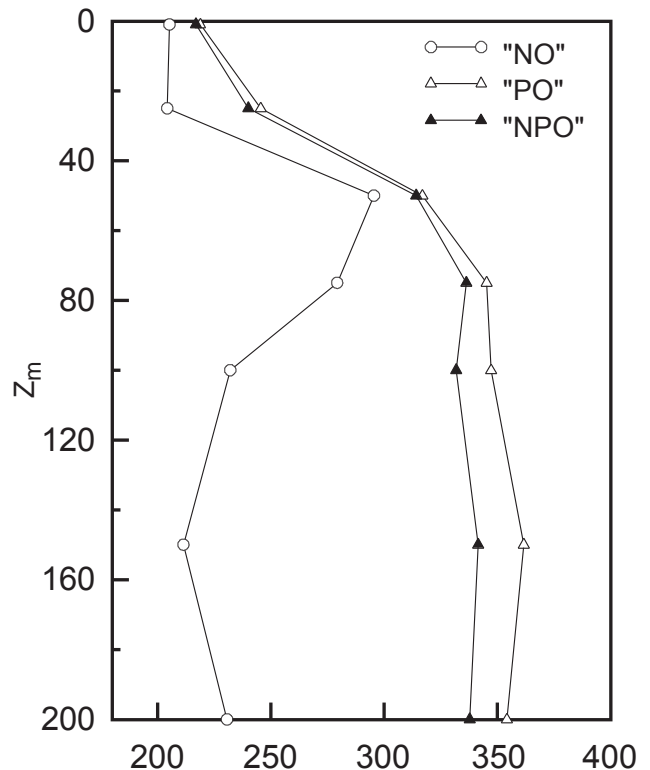


FIG. 9. – Vertical distribution of “NO”, “PO”, and “NPO” off Arabia during the intermonsoon period at the beginning of November, with abundant *Trichodesmium* mats at the surface.

Figure 9 presents the true values of “NO”, “PO”, and “NPO” at an oceanographic survey station where high levels of  $N_2$  fixation were recorded off eastern Arabia at the beginning of November, during a lull in between monsoons following the period of active upwelling driven by the SW monsoon, showing a prevalence of *Trichodesmium* (IIOE, 1965).  $O_2$  values ( $10 \mu\text{moles/kg}$ ) in the water layer below 80–100 m were very low, indicative of a source subject to heavy denitrification, borne out by the difference in the value of “PO”–“NO” below 100 m.

The quantity of  $N_2$  fixed in the upper layers is given by the Equation:

$$N_2 \text{ fixation} = (\Delta \text{“NO”} - \Delta \text{“PO”}) / (2 \cdot R_N) \quad (23)$$

where  $\Delta \text{“NO”}$  is, as always, the difference between “NO” at each level and “NO”<sub>D</sub> at the reference depth  $Z_D = 100$  m, and the same applies to the other two tracers. Equation 23 is independent of losses of  $O_2$  to the atmosphere and abnormal carbohydrate synthesis, if any. Both “NO” and “PO” vary with excess carbohydrate synthesis, but the variation is of the same order of magnitude, and hence the anomalies in those tracers cancel out.

Cumulative  $N_2$  fixation at this station in the Arabian Sea over the entire period from the start of the bloom was  $5.6 \mu\text{moles/kg}$  in the surface layer, with concurrent usage of  $74 \mu\text{moles/kg}$  of  $CO_2$ . Nitrate+nitrite at depths  $Z_D$  and 0 m was 24.5 and  $0.4 \mu\text{moles}$ , respectively, and yields a  $CO_2$  uptake value of  $160 \mu\text{moles/kg}$  when inserted in Equation 13, consistent with Redfield stoichiometry. This means that carbon fixation in the surface layer by *Trichodesmium* accounted for 32 % of total carbon fixation.

Heavy losses of  $O_2$  to the atmosphere were also observed from the shift in the “NPO” value towards lower values. When migratory dinoflagellates are not present,  $O_2$  losses are equal to  $\Delta \text{“NPO”}$ , which is  $115 \mu\text{moles/kg}$  in the surface layer. The losses are consistent with the total balance of  $O_2$  production, namely,  $O_2$  produced according to Redfield stoichiometry until depletion of  $NO_3$  plus that produced according to Equation 8.

Patterns may become more complicated during transitions from one population to another. At such times populations of migratory dinoflagellates may occasionally coexist with populations of cyanobacteria. In such cases tracer “NPO” ceases to be con-

servative, but “NPCO” continues to be conservative and can still be used, even in those conditions. This latter tracer value enables the quantity of excess carbohydrate synthesis by the dinoflagellates to be calculated, namely,

$$C-C_{bh} = \Delta^{*}NPO - \Delta^{*}NPCO$$

In certain exceptional cases cyanobacterial populations may not follow the general pattern represented in Figure 8 at all. Margalef (1973) recorded the presence of *Ocillatoria thiebautii* off NW Africa between Cape Blanco and Cape Verde, and in an advance publication of preliminary results called attention to the fact that nitrogen was not in fact the limiting nutrient in that region (Margalef, 1971). This may have been due to inputs of phosphate by way of dust from the Sahara, which were quite intense during the survey in question. Such inputs of phosphate through the surface fall outside stoichiometric considerations.

## GENERAL CONSIDERATIONS

All the approaches to the Redfield ratio anomalies discussed above have assumed that the water masses in the photic and subphotic zones are uniform and that water composition was initially the same as the water at depth  $Z_D$  taken for reference purposes. The calculations described can also be applied in areas of stratification with lateral advection of water masses having differing features, provided that correction for mixing can be effected based on knowledge of the area's hydrography.

One general characteristic of the tracers described is that they are independent of losses through sedimentation of particulate matter or inputs of particles from upper levels and only reflect abnormalities in synthesis or mineralization processes within each layer.

The tracers are particularly appropriate for application to spatially decoupled biological processes taking place in different layers, such as the strategies employed by dinoflagellates and *Rhizosolenia*, which are difficult to reproduce in the laboratory.

Another advantage is that alterations in the marine environment as a result of abnormal biomass synthesis are cumulative, leaving behind a sort of record of what has happened in the environment. This is very useful when a bloom of the red tide type appears, since by the time it has been detected it is

already too late to collect data on the preceding days. This record remains until it is wiped away by turbulence.

These tracers are widely recognized to be useful in studying the transition from one phytoplankton population with a certain strategy for nutrient use to another phytoplankton population with a different strategy. The two populations exist side by side for a certain period of time, each producing a different sort of disturbance, as in the case when migratory dinoflagellates coexist with coccolithophores, or in certain special cases when dinoflagellates are replaced by cyanobacteria. The calculation mechanism discussed here allows the alterations produced concurrently by each population to be assessed separately.

Another subject area of discussion (Banse, 1974, 1994) is the  $\Delta CO_2 : \Delta NO_3$  ratio in the surface layers. As long as quantities of  $NO_3$  are present in the photic zone, the C:N ratio is the same as the Redfield ratio, but when the nutrients have been used up, the ratio value considerably exceeds 6.6. According to Equation 14, theoretically it tends towards infinity. In deep water the C:N ratio follows the Redfield ratio quite closely, but when there is a heavy bloom of migratory dinoflagellates in the water layer designated here as the subphotic layer between depths  $Z_C$  and  $Z_D$  and the nitrocline is at a depth below the 1% light level, the C:N ratio value is below 6.6 and during a red tide can fall to a value approaching zero (Ríos *et al.*, 1998).

In this respect, another highly topical issue is calculation of biomass production to determine carbon transport from the surface to the sea bed as a result of sedimentation of that biomass. The stoichiometry of biomass synthesis may furnish considerable information for interpreting the results. One aspect is whether excess carbohydrate synthesis, which is not included in the biomass calculated on the basis of nitrate consumption, should be added to the biomass calculation. In this respect, soluble carbohydrates are formed at the end of a diatom bloom, but that production is not exported to the sea bed, because these carbohydrates are broken down and oxidized within the same water mass where they were originally formed. The highest particulate carbohydrate production takes place during blooms of migratory dinoflagellates. Restricting our consideration to the photic zone, biomass production is the equivalent of  $NO_3$  consumption until depletion, plus carbohydrate production by the dinoflagellates. On the other hand, for the water column as a whole, namely, the photic zone and the subphotic zone, car-

bohydrates in the subphotic zone are consumed with  $\text{NO}_3$  to yield biomass with a C:N ratio of 6.6, whereby the carbohydrate is entirely used up and the total production in the water column is equivalent to the total  $\text{NO}_3$  consumed between the surface and depth  $Z_D$  (Fig. 2).

## ACKNOWLEDGEMENTS

The author wishes to thank F.F. Pérez, F.G. Figueiras, A.F. Ríos, and X.A. Alvarez-Salgado of the Instituto de Investigaciones Marinas (CSIC) [Marine Research Institute] in Vigo for their helpful suggestions which greatly improved the manuscript of this paper. Ms. Trini Rellán plotted the Figures, and Mr. R. Sacks prepared the English translation from the original Spanish and M. Estrada revised it.

## REFERENCES

- Alvarez-Salgado, X.A., G. Rosón, F.F. Pérez and Y. Pazos. – 1993. Hydrographic variability off the Rías Baixas (NW Spain) during the upwelling season. *J. Geophys. Res.*, 98: 14447-14455.
- Anderson, L.A. – 1995. On the hydrogen and oxygen content of marine phytoplankton. *Deep-Sea Res.*, 42: 1675-1680.
- Balch, W.M., J. Fritz and E. Fernandez. – 1996. Decoupling of calcification and photosynthesis in the coccolithophore *Emiliania huxleyi* under steady-state light-limited growth. *Mar. Ecol. Progr. Ser.*, 142: 87-97.
- Banase, K. 1974.- On the interpretation of data for the carbon-to-nitrogen ratio of phytoplankton. *Limnol. Oceanogr.* 19:695-699.
- Banase, K. – 1994. Uptake of inorganic carbon and nitrate by marine plankton and the Redfield ratio. *Global Biogeochemical Cycles*, 8(1): 81-84.
- Broecker, W.S. – 1974. "NO", a conservative water-mass tracer. *Earth and Planetary Science Letters*, 23: 100-107.
- Buitenhuis, E.T., H.J.W. de Baar and M.J.W. Veldhuis. – 1999. Photosynthesis and calcification by *Emiliania huxleyi* (prymnesiophyceae) as a function of inorganic carbon species. *J. Phycol.*, 35: 949-959.
- Cullen, J.J. – 1985. Diel vertical migration by dinoflagellates: roles of carbohydrate metabolism and behavioral flexibility. *Mar. Sci.*, 27: 135-152.
- Cullen, J.J., M. Zhu, R.F. Davis and D.C. Pierson. – 1985. Vertical migration, carbohydrate synthesis, and nocturnal nitrate uptake during growth of *Heterocapsa niei* in laboratory water column. In: Anderson, White and Baden. *Toxic Dinoflagellates*. pp. 189-194. Elsevier Science Publishing Co.
- Emerson, S. and T.L. Hayward. – 1995. Chemical tracers of biological processes in shallow waters of North Pacific: Preformed nitrate distributions. *J. Mar. Res.*, 53: 499-513.
- Fernández, E., W.M. Balch, E. Marañón and P.M. Holligan. – 1994. High rates of lipid biosynthesis in cultured, mesocosm and coastal populations of the coccolithophore *Emiliania huxleyi*. *Mar. Ecol.*, 114: 13-22.
- Fleming, R.H. – 1940. Composition of plankton and units for reporting populations and production. *Proc. Sixth Pacific Science Congress 1939*, 3: 535-540.
- Fraga, F., X.A. Alvarez-Salgado and F.F. Pérez. – On the variation of alkalinity during phytoplankton photosynthesis. (submitted.)
- Fraga, F. and F.F. Pérez. – 1990. Transformaciones entre composición química del fitoplancton, composición elemental y relación de Redfield. *Sci. Mar.*, 54(1): 69-76.
- Fraga, F., F.F. Pérez, F.G. Figueiras and A.F. Ríos. – 1992. Stoichiometric variations of N, P, C and  $\text{O}_2$  during a *Gymnodinium catenatum* red tide and their interpretation. *Mar. Ecol. Progr. Ser.*, 87: 123-134.
- Fraga, F., A.F. Ríos, F.F. Pérez, M. Estrada and C. Marrasé. – 1999. Effect of upwelling pulses on excess carbohydrate synthesis as deduced from nutrient, carbon dioxide and oxygen profiles. *Mar. Ecol. Progr. Ser.*, 189: 65-75.
- Fraga, F., A.F. Ríos, F.F. Pérez and F.G. Figueiras. – 1998. Theoretical limits of oxygen:carbon and oxygen:nitrogen ratios during photosynthesis and mineralisation of organic matter in the sea. *Sci. Mar.*, 62: 161-168.
- Goldman, J.C., D.A. Hansell and M.R. Dennett. – 1992. Chemical characterization of three large oceanic diatoms: potential impact on water column chemistry. *Mar. Ecol. Progr. Ser.*, 88: 257-270.
- Holligan, P.M., E. Fernández, J. Aiken, W.M. Balch, P. Boyd, P.H. Burkill, M. Finch, S.B. Groom, G. Malin, K. Muller, D.A. Purdie, C. Robinson, C.C. Trees, S.M. Turner and P. van der Wal. – 1993. A biogeochemical study of the coccolithophore, *Emiliania huxleyi*, in the North Atlantic. *Global Biogeochemical Cycles*, 7: 879-900.
- IIOE. – 1965. *International Indian Ocean Expedition. Final cruise report 'Anton Bruun' cruises 4A and 4B*. Ed. Woods Hole Oceanographic Institution.
- Laws, E.A. – 1991. Photosynthetic quotients, new production and net community production in the open ocean. *Deep-Sea Res.*, 38: 143-167.
- Marañón, E. and N. González. – 1997. Primary production, calcification and macromolecular synthesis in a bloom of the coccolithophore *Emiliania huxleyi* in the North Sea. *Mar. Ecol. Progr. Ser.*, 157: 61-77.
- Margalef, R. – 1971. Una campaña oceanográfica del Cornide de Saavedra en la región de afloramiento del noroeste africano. *Invest. Pesq.*, Barcelona, 35: 1-39.
- Margalef, R. – 1973. Fitoplancton marino de la región de afloramiento del NW de Africa. *Res. Exp. Cient. B/O Cornide*, 2: 65-94.
- Margalef, R. – 1978. Life forms of phytoplankton as survival alternatives in an unstable environment. *Oceanol. Acta*, 1: 493-509.
- Miyata, K. and A. Hattori. – 1986. A simple fractionation method for determination of phosphorus components in phytoplankton: Application to natural populations of phytoplankton in summer surface waters of Tokyo Bay. *J. Ocean. Soc. Japan*, 42: 255-265.
- Moore, J.K. and T.A. Villareal. – 1996. Buoyancy and growth characteristics of three positively buoyant marine diatoms. *Mar. Ecol.*, 132: 203-213.
- Paasche, E. – 1998. Roles of nitrogen and phosphorus in coccolith formation in *Emiliania huxleyi* (Prymnesiophyceae). *Eur. J. Phycol.*, 33: 33-42.
- Redfield, A.C., B.K. Ketchum and F.A. Richards. – 1963. The influence of organisms on the composition of sea-water. In: M.N. Hill. *The Sea*. Vol. 2, pp. 26-77. Wiley, New York.
- Richardson, T.L., A.M. Ciotti, J.J. Cullen and T.A. Villareal. – 1996. Physiological and optical properties of *Rhizosolenia* forma (Bacillariophyceae) in the context of open-ocean vertical migration. *J. Phycol.*, 32: 417-757.
- Richardson, T.L. and J.J. Cullen. – 1995. Changes in buoyancy and chemical composition during growth of a coastal marine diatom: ecological and biogeochemical consequences. *Mar. Ecol.*, 128: 77-99.
- Richardson, T.L., J.J. Cullen, D.E. Kelley and M.R. Lewis. – 1998. Potential contributions of vertical migrating *Rhizosolenia* to nutrient cycling and production in the open ocean. *J. Plankton Res.*, 20: 219-241.
- Ríos, A.F., F. Fraga, F.G. Figueiras and F.F. Pérez. – 1998. A modelling approach to the Redfield ratio deviations in the ocean. *Sci. Mar.*, 62(1-2): 169-176.
- Robertson, J.E., C. Robinson, D.R. Turner, P. Holligan, A.J. Watson, P. Boyd, E. Fernandez and M. Finch. – 1994. The impact of a coccolithophore bloom on oceanic carbon uptake in the northeast Atlantic during summer 1991. *Deep-Sea Res.*, 41: 297-314.
- Sambrotto, R.N., G. Savidge, C. Robinson, P. Boyd, T. Takahashi, D.M. Kari, C. Langdon, D. Chipman, J. Marra and L. Codispoti. – 1993. Elevated consumption of carbon relative to nitrogen in the surface ocean. *Nature*, 363: 248-250.
- Taguchi, S., J.A. Hirata and E.A. Laws. – 1987. Silicate deficiency and lipid synthesis of marine diatoms. *J. Phycol.*, 23: 260-267.
- Villareal, T.A., M.A. Altabet and K. Culver-Rymsza. – 1993. Nitro-



gen transport by vertically migrating diatom mats in the North Pacific Ocean. *Nature*, 363: 709-712.

Villareal, T.A., C. Pilskaln, M. Brzezinski, F. Lipschultz, M. Dennett and G.B. Gardner. – 1999. Upward transport of oceanic nitrate by migrating diatom mats. *Nature*, 397: 423-425.

Villareal, T.A., S. Woods, J.K. Moore and K. Culver-Rymsza. – 1996. Vertical migration of *Rhizosolenia* mats and their significance to  $\text{NO}_3^-$  fluxes in the central North Pacific gyre. *J. Plankton Res.*, 18: 1103-1121.

Vollenweider, R.A., G. Montanari and A. Rinaldi. – 1995. Statistical inferences about the mucilage events in the Adriatic Sea, with special reference to recurrence patterns and claimed relationship to sun activity cycles. *The Science of the Total Environment*, 165: 213-224.

Williams, P.J.leB. – 1995. Evidence for the seasonal accumulation of carbon-rich dissolved organic material, its scale in comparison with changes in particulate material and the consequential effect on net C/N assimilation ratios. *Mar. Chem.*, 51:17-29.

## ANNEX I

Introduction of the terms  $\text{NH}_4^+$  and  $\text{NO}_2^-$ , as well as  $\text{NO}_3^-$ , in the equation in the text of the paper causes  $A_p$  to remain constant even though photosynthesis goes on at the expense of nitrate, ammonia, nitrite, or any combination of these in any proportion. The coefficient 0.5 for nitrite is the proportion of dissociated nitrite at pH 4.4.

The changes in alkalinity brought about by photosynthesis have been considered in detail in a paper by F. Fraga *et al.* (in press). The results presented in that paper that are of interest here are summarized below.

The equation for potential alkalinity is, in full:

$$A_p = A_T + \text{NO}_3^- - \text{NH}_4^+ + 0.5 \text{NO}_2^- + 0.23 \text{HPO}_4^{2-} + 0.074 \text{DIN}$$

DIN (Dissolved Inorganic Nitrogen,  $\text{NO}_3^- + \text{NH}_4^+ + \text{NO}_2^-$ ).

Phosphate is present in organic matter in the form of esters or diesters with sugar molecules, hence it remains a strong monoacid. For that reason, no change in alkalinity is to be expected. On the other hand, synthesized organic molecules containing basic groups are also bound to the phosphate, and these increase the alkalinity. In addition, formation of basic amino acids also goes on along with consumption of sulphur for protein synthesis, at a rate proportional to the total assimilated nitrogen. The preceding equation is valid for all N:P ratios.

In the case of cyanobacteria, when  $\text{N}_2$  fixation takes place the  $\text{N}_2$  has to be included in the DIN, but this can be offset by replacing the DIN by phosphate multiplied by the N:P ratio for the biomatter. Assigning the value 16:1, the equation takes the form:

$$A_p = A_T + \text{NO}_3^- - \text{NH}_4^+ + 0.5 \text{NO}_2^- + 1.43 \text{HPO}_4^{2-}$$

which is also valid for the other cases, provided that the N:P ratio is as just indicated above.

When coccolithophores are present and precipitation of  $\text{CaCO}_3$  takes place, the sample should be filtered, as discussed in the text of the paper. In this case, a separate correction should be made for phytoplankton alkalinity. The equation for filtered seawater after photosynthesis is:

$$A_p = A_T + \text{NO}_3^- - \text{NH}_4^+ + 0.5 \text{NO}_2^- - 0.25 \text{HPO}_4^{2-} + 0.016 \text{DIN}$$

Thus, variations in  $A_p$  are attributable solely to the formation or dissolution of  $\text{CaCO}_3$ . For an N:P ratio value = 16:1, the preceding equation can practically be reduced to:

$$\text{Filtered water: } A_p = A_T + \text{NO}_3^- - \text{NH}_4^+ + 0.5 \text{NO}_2^-$$

The tracers that include  $A_p$  are ordinarily used when coccolithophores are present and the samples have to be filtered, and thus this last equation is the most appropriate equation for use in this case.